

F-TERM HYBRID INFLATION AND SUSY BREAKING

C. PALLIS

*School of Civil Engineering,
Faculty of Engineering,
Aristotle University of Thessaloniki,
GR-541 24 Thessaloniki, GREECE
E-mail: kpallis@auth.gr*

ABSTRACT: We consider F-term hybrid inflation and supersymmetry breaking in the context of a model which largely respects a global $U(1)$ R symmetry. The Kähler potential parameterizes the Kähler manifold with an enhanced $U(1)_R \times (SU(1,1)/U(1))$ symmetry, where the scalar curvature of the second factor is determined by the achievement of a supersymmetry-breaking de Sitter vacuum without ugly tuning. The magnitude of the emergent soft tadpole term for the inflaton can be adjusted in the range $(1.2 - 460)$ TeV – increasing with the dimensionality of the representation of the waterfall fields – so that the inflationary observables are in agreement with the observational requirements. The mass scale of the supersymmetric partners turns out to lie in the region $(0.09 - 253)$ PeV which is compatible with high-scale supersymmetry and the results of LHC on the Higgs boson mass. The μ parameter can be generated by conveniently applying the Giudice-Masiero mechanism and assures the out-of-equilibrium decay of the R saxion at a low reheat temperature $T_{\text{rh}} \leq 163$ GeV.

1. MOTIVATION

The *Supersymmetric* (SUSY) hybrid inflation [1] based on F terms, called for short henceforth *F-term hybrid inflation* (FHI) is undoubtedly a well-motivated, flexible and easily embedded in Particle models inflationary model for a number of reasons. Most notably:

- It is based on a renormalizable superpotential uniquely determined by a gauge \mathbb{G} and a global $U(1)$ R symmetries;
- It does not require fine tuned parameters and transplanckian inflaton values;
- It can be naturally followed by a *Grand Unified Theory* (GUT) phase transition which may lead to the production of cosmological defects, if these are predicted by the symmetry-breaking scheme.

However, the original version of FHI [1], which employs only *radiative corrections* (RCs) into the inflationary potential is considered as strongly disfavored by the *Planck* data [2] due to the large scalar spectral index. This conclusion can be evaded, if we take in to account soft SUSY-breaking terms [3–5] and *Supergravity* (SUGRA) corrections [6] with appropriate magnitude. Both corrections above are related to the adopted SUSY-breaking or *hidden sector* (HS) sector of the theory. Therefore, it is crucial to obtain a consistent interconnection of HS with the *inflationary sector* (IS) of FHI.

A possible combination of the aforementioned sectors is presented in Sec. 2 following Ref. [7] – see also Ref. [8]. Then, in Sec. 3 we reconcile the inflationary observables with data and describe the post-inflationary evolution in Sec. 4 which is related to the *Dark Energy* (DE) problem, the immunity of *Big Bang Nucleosynthesis* (BBN) from the notorious moduli problem and the *Gravitational Waves* (GWs) obtained from the decay of *Cosmic Strings* (CSs). Our conclusions are summarized in Sec. 5.

2. LINKING FHI WITH A SUSY-BREAKING SECTOR

To achieve a consistent combination of HS and IS we use the R symmetry, which is a crucial ingredient for the implementation of FHI, as a junction mechanism. Below we specify the particle content, the superpotential, and the Kähler potential of our model in Secs. 2.1, 2.2 and 2.3 respectively.

2.1 PARTICLE CONTENT

FHI can be implemented by introducing three superfields $\bar{\Phi}$, Φ and S . The two first are left-handed chiral superfields oppositely charged under a gauge group \mathbb{G} whereas the latter is the inflaton and is a \mathbb{G} -singlet left-handed chiral superfield. Singlet under \mathbb{G} is also the SUSY breaking (goldstino) superfield Z . In this work we identify \mathbb{G} with three possible gauge groups with different dimensionalities N_G of the representations to which $\bar{\Phi}$ and Φ belong – see Table 1. Namely, we consider the following \mathbb{G} 's

$$\mathbb{G}_{B-L} := \mathbb{G}_{SM} \times U(1)_{B-L} \quad \text{with } N_G = 1, \quad (2.1a)$$

$$\mathbb{G}_{LR} := SU(3)_C \times SU(2)_L \times SU(2)_R \times U(1)_{B-L} \quad \text{with } N_G = 2, \quad (2.1b)$$

$$\mathbb{G}_{5_X} := SU(5) \times U(1)_X \quad \text{with } N_G = 10. \quad (2.1c)$$

Here \mathbb{G}_{SM} is the well-known gauge group of the SM

$$\mathbb{G}_{SM} := SU(3)_C \times SU(2)_L \times U(1)_Y, \quad (2.1d)$$

SUPER- FIELDS	REPRESENTATIONS UNDER \mathbb{G}			R
	\mathbb{G}_{B-L}	\mathbb{G}_{LR}	$\mathbb{G}_{5_{\mathbf{x}}}$	CHARGE
HIGGS SUPERFIELDS				
Φ	$(\mathbf{1}, \mathbf{1}, 0, 2)$	$(\mathbf{1}, \mathbf{1}, \mathbf{2}, 1)$	$(\mathbf{10}, 1)$	0
$\bar{\Phi}$	$(\mathbf{1}, \mathbf{1}, 0, -2)$	$(\mathbf{1}, \mathbf{1}, \bar{\mathbf{2}}, -1)$	$(\bar{\mathbf{10}}, -1)$	0
S	$(\mathbf{1}, \mathbf{1}, 0, 0)$	$(\mathbf{1}, \mathbf{1}, \mathbf{1}, 0)$	$\mathbf{1}$	2
GOLDSTINO SUPERFIELD				
Z	$(\mathbf{1}, \mathbf{1}, 0, 0)$	$(\mathbf{1}, \mathbf{1}, \mathbf{1}, 0)$	$\mathbf{1}$	$2/\nu$

TABLE 1: Representations and R charges of the superfields involved in the IS and HS for the various \mathbb{G} 's.

to which \mathbb{G} is broken via the *vacuum expectation values* (v.e.vs) of Φ and $\bar{\Phi}$ at the end of FHI. As regards the cosmological defects, CSs are produced only for $\mathbb{G} = \mathbb{G}_{B-L}$ – see Sec. 4.4.

2.2 SUPERPOTENTIAL

The superpotential of our model carries R charge 2 and is linear *with respect to* (w.r.t.) S and Z^ν . It naturally splits into four parts:

$$W = W_I + W_H + W_{GH} + W_Y, \quad (2.2)$$

where the subscripts “I” and “H” stand for the IS and HS respectively and the content of each term is specified as follows:

- (a) W_I is the part of W related to IS [1]:

$$W_I = \kappa S (\bar{\Phi}\Phi - M^2), \quad (2.3a)$$

where κ and M are free parameters which may be constrained by the inflationary requirements – see Sec. 3.4.

- (b) W_H is the part of W devoted to HS [9]:

$$W_H = m m_P^2 (Z/m_P)^\nu, \quad (2.3b)$$

where $m_P = 2.4$ ReV is the reduced Planck mass – with $\text{ReV} = 10^{18}$ GeV –, m is a positive free parameter with mass dimensions, and ν is an exponent which may, in principle, acquire any real value if W_H is considered as an effective superpotential valid close to non-zero $\langle Z \rangle$. We assume though that $\nu > 0$. If we also assume that W is holomorphic in S then mixed terms of the form $S^{\nu_s} Z^{\nu_z}$ can be forbidden in W since the exponent of a such term has to obey the relation

$$\nu_s + \nu_z/\nu = 1 \Rightarrow \nu_z = (1 - \nu_s)\nu,$$

leading to negative values of ν_z . This conclusion contradicts with our assumptions above.

SUPER-FIELDS	REPRESENTATIONS UNDER \mathbb{G}			R CHARGE
	\mathbb{G}_{B-L}	\mathbb{G}_{LR}	\mathbb{G}_{5_X}	
H_u	$(\mathbf{1}, \mathbf{2}, 1/2, 0)$			2
H_d	$(\mathbf{1}, \mathbf{2}, -1/2, 0)$			2
\mathbf{h}		$(\mathbf{1}, \mathbf{2}, \mathbf{2}, 0)$		2
$\mathbf{5}_h$			$(\mathbf{5}, 2)$	2
$\bar{\mathbf{5}}_h$			$(\bar{\mathbf{5}}, -2)$	2

TABLE 2: Representations and R charges of the electroweak Higgs superfields for the various \mathbb{G} 's.

(c) W_{GH} is a term which mixes Z and $\bar{\Phi} - \Phi$

$$W_{GH} = -\lambda m_P (Z/m_P)^\nu \bar{\Phi} \Phi \quad (2.3c)$$

with λ a real coupling constant. The magnitude of λ can be restricted by the DE requirement as we see in Sec. 4.1 below.

(d) W_Y includes the usual trilinear terms with Yukawa couplings between the various superfields of *Minimal SUSY Standard Model* (MSSM), denoted by Y_α with $\alpha = 1, \dots, 7$, i.e.,

$$Y_\alpha = Q, L, d^c, u^c, e^c, H_d, \text{ and } H_u,$$

where the generation indices are suppressed. Note, however, that the R assignments as shown in Table 2 for the electroweak Higgs superfields prohibit the presence in W of a bilinear term of the form

$$H_B = \begin{cases} H_u H_d & \text{for } \mathbb{G} = \mathbb{G}_{B-L}, \\ \mathbf{h}^2 & \text{for } \mathbb{G} = \mathbb{G}_{LR}, \\ \bar{\mathbf{5}}_h \mathbf{5}_h & \text{for } \mathbb{G} = \mathbb{G}_{5_X}. \end{cases} \quad (2.4)$$

and other unwanted mixing terms – e.g. $\lambda_\mu S H_u H_d$, $\lambda Z^\nu H_u H_d / m_P^\nu$. We do not address the issue of the generation of tiny neutrino masses here – see Ref. [8].

2.3 KÄHLER POTENTIAL

The Kähler potential respects the adopted \mathbb{G} symmetry in Table 1. It has the following contributions

$$K = K_I + K_H + K_\mu + |Y_\alpha|^2, \quad (2.5)$$

which can be specified as follows:

(a) K_I depends on the fields involved in FHI – cf. Eq. (2.3a). We adopt the simplest possible choice [4, 6] that has the form

$$K_I = |S|^2 + |\Phi|^2 + |\bar{\Phi}|^2. \quad (2.6a)$$

Higher order terms of the form $|S|^{2\nu_S} / m_P^{2\nu_S-2}$ with $\nu_S > 1$ can not be excluded by the imposed symmetries but may become harmless if $S \ll m_P$ and assume low enough coefficients.

(b) K_H is devoted to HS. We adopt the form introduced in Ref. [9] where

$$K_H = Nm_{\text{P}}^2 \ln \left(1 + \frac{|Z|^2 - k^2 Z_{\pm}^4 / m_{\text{P}}^2}{Nm_{\text{P}}^2} \right) \quad \text{with } Z_{\pm} = Z \pm Z^*. \quad (2.6b)$$

Here, $k > 0$ mildly violates R symmetry endowing R axion with phenomenologically acceptable mass. The selected K_H is largely respects the R symmetry, which is a crucial ingredient for FHI, and it ensures – as we see in Sec. 4.1 – a dS vacuum of the whole field system with tunable cosmological constant for

$$N = \frac{4v^2}{3-4v} \quad \text{with } \frac{3}{4} < v < \frac{3}{2} \quad \text{for } N < 0. \quad (2.7)$$

Our favored v range finally is $3/4 < v < 1$. Since $N < 0$, K_H parameterizes the $SU(1,1)/U(1)$ hyperbolic Kähler manifold for $k \sim 0$.

(c) K_{μ} includes higher order terms which generate the needed mixing term between H_u and H_d in the lagrangian of MSSM [9] and has the form

$$K_{\mu} = \lambda_{\mu} \left(Z^{*2v} / m_{\text{P}}^{2v} \right) H_B + \text{h.c.}, \quad (2.8)$$

where the dimensionless constant λ_{μ} is taken real for simplicity.

The total K in Eq. (2.5) enjoys an enhanced symmetry for the \bar{Y}_A, S and Z fields with $\bar{Y}_A = Y_{\alpha}, \bar{\Phi}, \Phi, S$. Namely,

$$\prod_A U(1)_{\bar{Y}_A} \times (SU(1,1)/U(1))_Z, \quad (2.9)$$

where the indices indicate the moduli which parameterize the corresponding manifolds. Thanks to this symmetry, mixing terms of the form $S^{\tilde{v}_s} Z^{*\tilde{v}_z}$ can be ignored although they may be allowed by the R symmetry for $\tilde{v}_z = v\tilde{v}_s$. Most notably, $U(1)_S$ protects K_I from S depended terms which violates the R symmetry, thereby, spoiling the inflationary set-up.

3. INFLATION ANALYSIS

It is well known [1, 6] that in global SUSY FHI takes place for $|S| \gg M$ along a F- and D- flat direction of the SUSY potential

$$\bar{\Phi} = \Phi = 0, \quad \text{where } V_{\text{SUSY}}(\Phi = 0) := V_{I0} = \kappa^2 M^4 \quad \text{and } H_I = \sqrt{V_{I0}/3m_{\text{P}}^2} \quad (3.1)$$

are the constant potential energy density and the corresponding Hubble parameter which drive FHI – the subscript 0 means that this is the tree level value. The same configuration can be used as an inflationary track [7] if we consider the SUGRA F-term potential V_F and stabilize the HS of the model – see Sec. 3.1. Then, in Sec. 3.2, we give the form of the inflationary potential and employ it to obtain our results presented in Sec. 3.4 after imposing a number of constraints listed in Sec. 3.3.

\mathbb{G}	$\lambda/10^{-12}$	M/TeV	m/PeV	α_s/TeV
\mathbb{G}_{B-L}	0.2	1.4	0.5	2.63
\mathbb{G}_{LR}	1.7	1.9	1.15	6.7
\mathbb{G}_{5_X}	2.6	3.6	6.3	56.3

TABLE 3: Parameters of interest for the various \mathbb{G} 's with fixed $\kappa = 5 \cdot 10^{-4}$, $\nu = 7/8$ and $k = 0.1$ resulting to $n_s = 0.967$ – recall that $1 \text{ TeV} = 10^{15} \text{ GeV}$.

3.1 HIDDEN SECTOR'S STABILIZATION

FHI may be attained if Z is well stabilized during it to a value well below m_P . To determine this, we analyze the relevant fields as follows

$$Z = (z + i\theta)/\sqrt{2} \quad \text{and} \quad S = \sigma e^{i\theta_S/m_P}/\sqrt{2} \quad (3.2)$$

and we construct [7] the complete expression for V_F along the inflationary trajectory in Eq. (3.1). Upon expanding the resulting expression for low S/m_P values and keeping $\theta = 0$ as in its present vacuum – see Sec. 4.1 below – we find that V_F is minimized for the value [7]

$$\langle z \rangle_I \simeq \left(\sqrt{3} \cdot 2^{\nu/2-1} H_I / m \nu \sqrt{1-\nu} \right)^{1/(\nu-2)} m_P. \quad (3.3)$$

Note that $\nu < 1$ assures a real value of $\langle z \rangle_I$ with $\langle z \rangle_I \ll m_P$ since $H_I/m \ll 1$. In particular, for the inputs of Table 3 we obtain $\langle z \rangle_I / 10^{-3} m_P = 1.1, 1.5$ and 2.5 for $\mathbb{G} = \mathbb{G}_{B-L}, \mathbb{G}_{LR}$ and \mathbb{G}_{5_X} respectively. Furthermore, $\langle z \rangle_I$ turns out to be independent from σ as highlighted in Fig. 1 where the quantity $10^5 (V_F / \kappa^2 M^4 - 1)$ is plotted as a function of z and σ with fixed $\theta = 0$ for the inputs of Table 3 with $\mathbb{G} = \mathbb{G}_{LR}$. We also depict by a thick black point the location of $(\langle z \rangle_I, \sigma_*)$, where σ_* is the value of σ when the pivot scale $k_* = 0.05/\text{Mpc}$ crosses outside the horizon of FHI – see Sec. 3.4 below.

The (canonically normalized) components of sgoldstino, acquire masses squared, respectively,

$$m_{I_z}^2 \simeq 6(2-\nu)H_I^2 \quad \text{and} \quad m_{I_\theta}^2 \simeq 3H_I^2 - m^2 (8\nu^2 m_P^2 - 3\langle z \rangle_I^2) \frac{4\nu(1-\nu)m_P^2 + (1-96k^2\nu)\langle z \rangle_I^2}{2^{3+\nu}\nu m_P^{2\nu}\langle z \rangle_I^{2(2-\nu)}}, \quad (3.4a)$$

whereas the mass of \tilde{G} turns out to be

$$m_{13/2} \simeq \left(\nu(1-\nu)^{1/2} m^2 / \nu / \sqrt{3} H_I \right)^{\nu/(2-\nu)}. \quad (3.4b)$$

Given that $H_I \sim \text{EeV}$ and taking into account the results arranged in the Table of Fig. 1 we can infer that $m_{I_z} \gg H_I$ and so z is well stabilized during FHI whereas $m_{I_\theta} \simeq H_I$ and gets slightly increased as k increases beyond 0.1. Therefore, no problem with the isocurvature perturbation is expected.

3.2 INFLATIONARY POTENTIAL

Expanding V_F for low S values, introducing the canonically normalized inflaton $\sigma = \sqrt{2}|S|$ and taking into account the RCs [1] we derive [7] the inflationary potential V_I which may take the form

$$V_I \simeq V_{I0} (1 + C_{RC} + C_{SSB} + C_{SUGRA}). \quad (3.5)$$

The individual contributions are specified as follows:

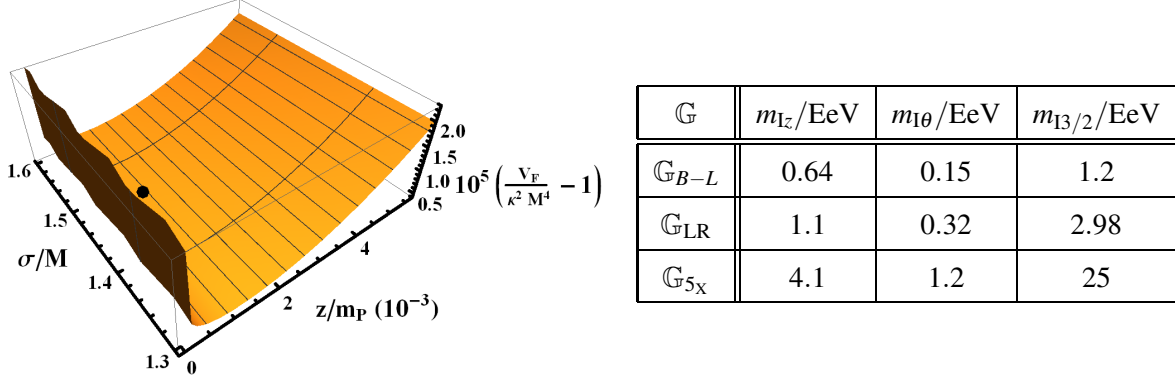


FIGURE 1: The SUGRA potential $10^5(V_F/\kappa^2 M^4 - 1)$ along the path in Eq. (3.1) as a function of z and σ for $\theta = 0$ and the parameters of Table 3 for $\mathbb{G} = \mathbb{G}_{LR}$. The location of $(\langle z \rangle_I, \sigma_*)$ is also depicted by a thick black point. The particle mass spectrum during FHI for the various \mathbb{G} 's are given in the Table – recall that $1 \text{ EeV} = 10^9 \text{ GeV}$.

(a) C_{RC} represents the RCs to V_I/V_{I0} which may be written as [1, 6]

$$C_{RC} = \frac{\kappa^2 N_G}{128\pi^2} \left(8 \ln \frac{\kappa^2 M^2}{Q^2} + f_{RC} \left(\frac{\sigma}{M} \right) \right) \quad \text{with } N_G = \begin{cases} 1 & \text{for } \mathbb{G} = \mathbb{G}_{B-L}, \\ 2 & \text{for } \mathbb{G} = \mathbb{G}_{LR}, \\ 10 & \text{for } \mathbb{G} = \mathbb{G}_{5_X}. \end{cases} \quad (3.6a)$$

Also the function f_{RC} may be expressed as

$$f_{RC}(x) = 8x^2 \tanh^{-1}(2/x^2) - 4(\ln 4 - x^4 \ln x) + (4 + x^4) \ln(x^4 - 4) \quad \text{with } x > \sqrt{2}. \quad (3.6b)$$

When σ tends to a critical value $\sigma_c = \sqrt{2}M$, the term including \tanh^{-1} tends to infinity. This means that one effective mass of the particle spectrum becomes negative, causing a destabilization of $\bar{\Phi}$ and Φ from zero in Eq. (3.1) triggering, thereby, the \mathbb{G} phase transition.

(b) C_{SSB} is the contribution to V_I/V_{I0} from the soft SUSY-breaking effects [3] parameterized as follows:

$$C_{SSB} = m_{13/2}^2 \sigma^2 / 2V_{I0} - a_S \sigma / \sqrt{2V_{I0}}, \quad (3.6c)$$

where the tadpole parameter reads [7]

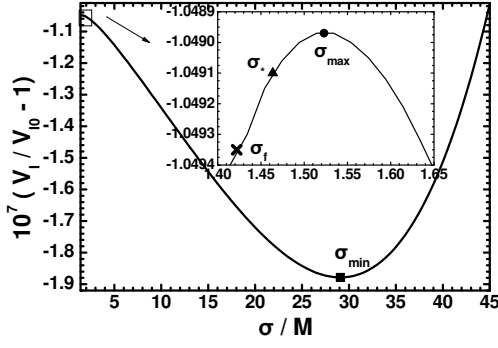
$$a_S = 2^{1-\nu/2} m \frac{\langle z \rangle_I^\nu}{m_P^\nu} \left(1 + \frac{\langle z \rangle_I^2}{2N m_P^2} \right) \left(2 - \nu - \frac{3\langle z \rangle_I^2}{8\nu m_P^2} \right). \quad (3.6d)$$

The minus sign results from the stabilization of θ at zero and the minimization of the factor $(S + S^*) = \sqrt{2}\sigma \cos(\theta_S/m_P)$ which occurs for $\theta_S/m_P = \pi \pmod{2\pi}$ – the decomposition of S is shown in Eq. (3.2). We further assume that θ_S remains constant during FHI so that the simple one-field slow-roll approximation is valid – cf. Ref. [5].

(c) C_{SUGRA} is the SUGRA correction to V_I/V_{I0} , after subtracting the one in C_{SSB} , which is [7]

$$C_{SUGRA} = c_{2\nu} \frac{\sigma^2}{2m_P^2} + c_{4\nu} \frac{\sigma^4}{4m_P^4} \quad \text{with } c_{2\nu} = \frac{\langle z \rangle_I^2}{2m_P^2} \quad \text{and } c_{4\nu} = \frac{1}{2} \left(1 + \frac{\langle z \rangle_I^2}{m_P^2} \right). \quad (3.6e)$$

The establishment of FHI is facilitated by the smallness of the coefficients above which is due to the minimality of K_I in Eq. (2.6a) and the stabilization of z at $\langle z \rangle_I \ll m_P$.



\mathbb{G}	$\sigma_*/\sqrt{2}M$	$\Delta_{c*} (\%)$	$\Delta_{\max*} (\%)$
\mathbb{G}_{B-L}	1.026	2.6	2.9
\mathbb{G}_{LR}	1.035	3.5	3.9
\mathbb{G}_{5_X}	1.067	6.7	7.3

FIGURE 2: The variation of V_I as a function of σ for the parameters given in Table 3 for $\mathbb{G} = \mathbb{G}_{LR}$. The values σ_* , σ_f , σ_{\max} , and σ_{\min} of σ are also depicted. Values of σ_* , Δ_{c*} and $\Delta_{\max*}$ for the inputs of Table 3 are also given in the Table for the various \mathbb{G} 's.

3.3 OBSERVATIONAL REQUIREMENTS

Our model of FHI can be qualified if we test it against a number of observational requirements. Namely:

- (a) The number of e-foldings that the pivot scale $k_* = 0.05/\text{Mpc}$ suffered during FHI have to be enough to resolve the problems of the Standard Big Bang, i.e., [2]:

$$N_{I*} = \int_{\sigma_f}^{\sigma_*} \frac{d\sigma}{m_p^2} \frac{V_I}{V_I'} \simeq 19.4 + \frac{2}{3} \ln \frac{V_{10}^{1/4}}{1 \text{ GeV}} + \frac{1}{3} \ln \frac{T_{\text{rh}}}{1 \text{ GeV}}, \quad (3.7)$$

where the prime denotes derivation w.r.t. σ , σ_* is the value of σ when k_* crosses outside the horizon of FHI and $\sigma_f \simeq \sigma_c$ signals the termination of FHI. Also we take for the reheating temperature T_{rh} a value close to those met in our set-up – see Sec. 4.2 below – $T_{\text{rh}} \simeq 1 \text{ GeV}$. In all cases, we obtain $N_{I*} \simeq 40$.

- (b) The amplitude A_s of the power spectrum of the curvature perturbation generated by σ during FHI must be appropriately normalized [10], i.e.,

$$A_s = \frac{1}{12 \pi^2 m_p^6} \frac{V_I^3(\sigma_*)}{|V_I'(\sigma_*)|^2} \simeq 2.105 \cdot 10^{-9}. \quad (3.8)$$

- (c) The remaining observables – the scalar spectral index n_s , its running α_s , and the scalar-to-tensor ratio r – which are calculated by the following standard formulas

$$n_s = 1 - 6\epsilon_* + 2\eta_*, \alpha_s = 2(4\eta_*^2 - (n_s - 1)^2)/3 - 2\xi_*, \text{ and } r = 16\epsilon_*, \quad (3.9)$$

(where $\xi \simeq m_p^4 V_I' V_I''' / V_I'^2$ and all the variables with the subscript $*$ are evaluated at $\sigma = \sigma_*$) must be in agreement with data, i.e., [2, 11]

$$n_s = 0.967 \pm 0.0074 \text{ and } r \lesssim 0.032, \quad (3.10)$$

at 95% confidence level (c.l.) with negligible $|\alpha_s| \ll 0.01$.

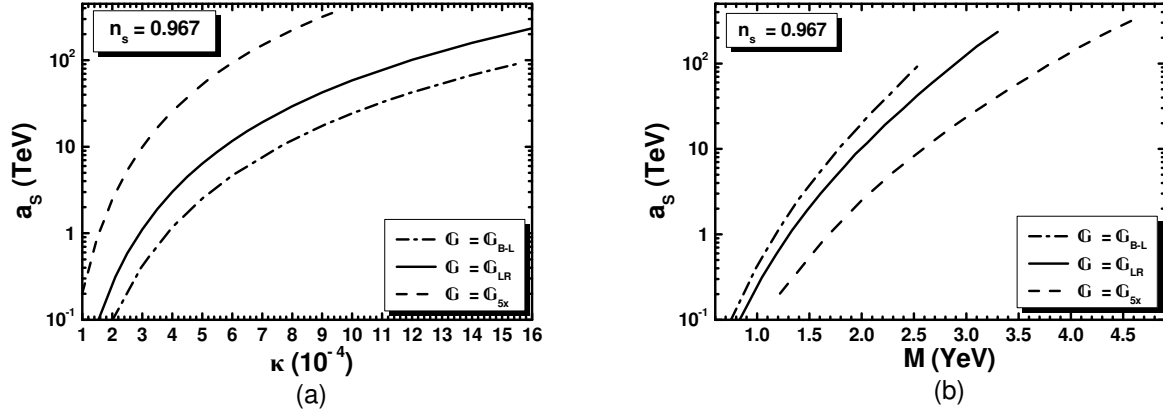


FIGURE 3: Values of a_s allowed by Eqs. (3.7), (3.8) and (3.10) versus κ (a) and M (b) for various \mathbb{G} 's and fixed $n_s = 0.967$.

3.4 RESULTS

Enforcing Eqs. (3.7) and (3.8) we can restrict M and σ_* as functions of κ for any given a_s . The correct values of n_s in Eq. (3.10) are attained if we carefully select a_s so that V_I in Eq. (3.5) becomes non-monotonic and develops a maximum at $\sigma = \sigma_{\max}$ and a minimum at $\sigma_{\min} \gg \sigma_{\max}$ as shown in Fig. 2. The relevant plot visualizes the variation of V_I as a function of σ for the parameters given in Table 3 with $\mathbb{G} = \mathbb{G}_{LR}$. From the subplot of this figure we remark that $\sigma_f < \sigma_* < \sigma_{\max}$ as suited for hilltop FHI [4, 5]. To qualify the relevant tuning we define the quantities

$$\Delta_{c*} = (\sigma_* - \sigma_c)/\sigma_c \text{ and } \Delta_{\max*} = (\sigma_{\max} - \sigma_*)/\sigma_{\max}. \quad (3.11)$$

The naturalness of the hilltop FHI increases with Δ_{c*} and $\Delta_{\max*}$. To get an impression of the amount of these tunings and their dependence on the parameters of the model, we display in the Table of Fig. 2 the resulting Δ_{c*} and $\Delta_{\max*}$ together with σ_* for the values of Table 3. We notice that $\Delta_{\max*} > \Delta_{c*}$ and that their values may be up to 10% increasing with N_G (and a_s). From our data we infer that $|\alpha_s| \sim 10^{-4}$ and $r \sim 10^{-11}$, and so beyond the reach of the planned experiments aiming to detect primordial GWs. For the n_s values in Eq. (3.10), we observe that r and $|\alpha_s|$ increase with a_s .

We also display in Fig. 3 the contours which are allowed by Eqs. (3.7) and (3.8) in the $\kappa - a_s$ and $M - a_s$ planes taking $n_s = 0.967$ and $\mathbb{G} = \mathbb{G}_{B-L}$ (dot-dashed line), $\mathbb{G} = \mathbb{G}_{LR}$ (solid line) and $\mathbb{G} = \mathbb{G}_{5x}$ (dashed line). The various lines terminate at κ values close to 10^{-3} beyond which no observationally acceptable inflationary solutions are possible. From the plotted curves we notice that the required a_s 's increase with N_G . In particular, we end up with the following ranges:

$$0.7 \lesssim M/\text{YeV} \lesssim 2.56 \text{ and } 0.1 \lesssim a_s/\text{TeV} \lesssim 100 \text{ for } \mathbb{G} = \mathbb{G}_{B-L}, \quad (3.12a)$$

$$0.82 \lesssim M/\text{YeV} \lesssim 3.7 \text{ and } 0.09 \lesssim a_s/\text{TeV} \lesssim 234 \text{ for } \mathbb{G} = \mathbb{G}_{LR}, \quad (3.12b)$$

$$1.22 \lesssim M/\text{YeV} \lesssim 4.77 \text{ and } 0.2 \lesssim a_s/\text{TeV} \lesssim 460 \text{ for } \mathbb{G} = \mathbb{G}_{5x}. \quad (3.12c)$$

The lower bounds of these inequalities are expected to be displaced to slightly larger values due to the BBN restrictions – see Sec. 4.2 below – which are not considered here for the shake of generality.

4. POST-INFLATIONARY CONSEQUENCES

We here explore the post-inflationary implications of our model related to the present vacuum – in Sec. 4.1 –, the commencement of the radiation dominated era – see Sec. 4.2 –, the SUSY scale – see Sec. 4.3 – and the observational consequences of CSs – see Sec. 4.4.

4.1 SUSY AND \mathbb{G} BREAKING – DARK ENERGY

The vacuum of our model is determined by minimizing the F-term (tree level) SUGRA scalar potential V_F derived [7] from W in Eq. (2.2) and K in Eq. (2.5). This lies along the D-flat direction $|\tilde{\Phi}| = |\Phi|$. Indeed, as verified numerically [7], V_F is minimized at the \mathbb{G} -breaking vacuum

$$|\langle\Phi\rangle| = |\langle\tilde{\Phi}\rangle| = M. \quad (4.1)$$

Substituting Eq. (3.2) in V_F and minimizing it w.r.t the various directions we arrive at the results

$$\langle\sigma\rangle \simeq 2^{(1-\nu)/2} (m - \lambda m_P) z^\nu / m_P^\nu \quad \text{and} \quad \langle z \rangle = 2\sqrt{2/3} |\nu| m_P, \quad (4.2)$$

which yield the constant potential energy density

$$\langle V_F \rangle \simeq \left(\frac{16\nu^4}{9} \right)^\nu \left(\frac{\lambda M^2 - m m_P}{\kappa m_P^2} \right)^2 \omega^N m_P^2 (\lambda m_P - m)^2 \quad \text{with} \quad \omega \simeq \frac{2(3-2\nu)}{3}. \quad (4.3)$$

Tuning λ to a value $\lambda \sim m/m_P \simeq 10^{-12}$ we may wish identify $\langle V_F \rangle$ with the DE energy density, i.e.,

$$\langle V_F \rangle = \Omega_\Lambda \rho_c = 7.3 \cdot 10^{-121} m_P^4, \quad (4.4)$$

where the density parameter of DE and the current critical energy density of the universe are respectively given by [10]

$$\Omega_\Lambda = 0.6889 \quad \text{and} \quad \rho_c = 2.31 \cdot 10^{-120} h^2 m_P^4 \quad \text{with} \quad h = 0.6766. \quad (4.5)$$

Therefore, we obtain a post-inflationary dS vacuum with $\langle\sigma\rangle \simeq 0$ which explains the notorious DE problem. The particle spectrum of the theory at the vacuum in Eqs. (4.1) and (4.2) includes the gravitino (\tilde{G}) with mass [9]

$$m_{3/2} = \langle e^{K_H/2m_P^2} W_H / m_P^2 \rangle \simeq 2^\nu 3^{-\nu/2} |\nu|^\nu m \omega^{N/2}, \quad (4.6a)$$

the IS with mass

$$m_I = e^{K_H/2m_P^2} \sqrt{2} (\kappa^2 M^2 + (4\nu^2/3)^\nu (1 + 4M^2/m_P^2) m^2)^{1/2}, \quad (4.6b)$$

which acquires some contribution from HS, the (canonically normalized) sgoldstino (or R saxion) and the pseudo-sgoldstino (or R axion) with respective masses

$$m_z \simeq 3\omega m_{3/2}/2\nu \quad \text{and} \quad m_\theta \simeq 12k\omega^{3/2} m_{3/2}. \quad (4.6c)$$

Numerical values for the masses above for the inputs of Table 3 are given in the Table of Fig. 4 for the various \mathbb{G} in Eqs. (2.1a) – (2.1c). Shown is also there the dimensionless SUGRA potential $V_F/m^2 m_P^2$ as a function of z and σ for the inputs of Table 3 and $\mathbb{G} = \mathbb{G}_{LR}$. The location of the dS vacuum in Eqs. (4.1) – (4.2) is depicted by a thick point.

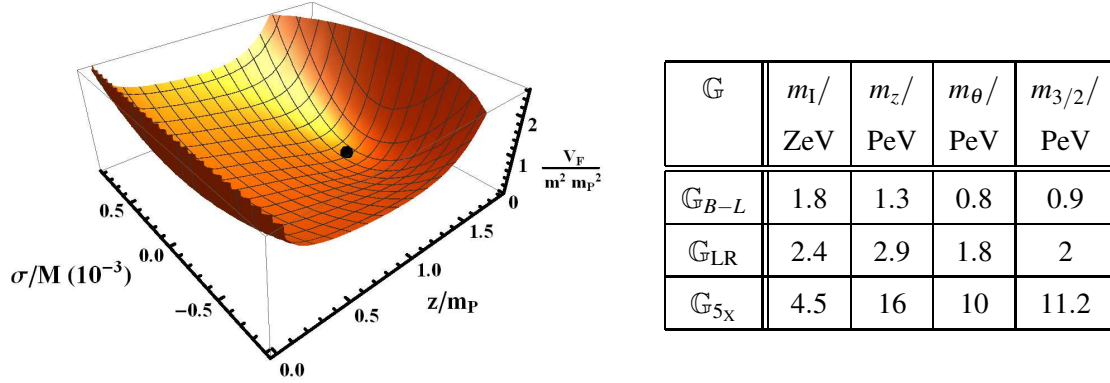


FIGURE 4: Dimensionless SUGRA potential V_F/m_P^2 as a function of z and σ for the inputs of Table 3 and $\mathbb{G} = \mathbb{G}_{LR}$. Shown is also the location of the dS vacuum in Eq. (4.1) and (4.2), depicted by a thick point. The particle mass spectra for the input of Table 3 are also given in the Table for the various \mathbb{G} 's considered – recall that $1 \text{ ZeV} = 10^{12} \text{ GeV} = 10^6 \text{ PeV}$.

At the vacuum of Eq. (4.2) K_μ in Eq. (2.8) gives rise to a non-vanishing μ term in the superpotential whereas the contributions W_Y and $|Y_\alpha|^2$ of W and K in Eqs. (2.2) and (2.5) lead to a common soft SUSY-breaking mass parameter \tilde{m} . Namely, we obtain [7, 9]

$$W \ni \mu H_u H_d \text{ with } |\mu| = \lambda_\mu (4v^2/3)^v (5 - 4v)m_{3/2} \text{ and } \tilde{m} = m_{3/2}. \quad (4.7)$$

The latter quantity indicatively represents the mass level of the SUSY partners.

4.2 REHEATING STAGE

After the termination of FHI, the IS and z start to oscillate about their minima in Eqs. (4.1) and (4.2) and eventually decay. When the Hubble rate becomes $H_{zI} \sim m_z$, the z condensate starts to dominate the universal energy budget, since the initial energy density of its oscillations ρ_{zI} is comparable to the energy density of the universe ρ_{zIt}

$$\rho_{zI} \sim m_z^2 \langle z \rangle^2 \text{ with } \langle z \rangle \sim m_P \text{ and } \rho_{zIt} = 3m_P^2 H_{zI}^2 \simeq 3m_P^2 m_z^2. \quad (4.8)$$

Due to the weakness of the gravitational interactions which govern the z decay, the reheating temperature

$$T_{rh} = (72/5\pi^2 g_{rh*})^{1/4} \Gamma_{\delta z}^{1/2} m_P^{1/2}, \text{ with } g_{rh*} \simeq 10.75 - 100 \quad (4.9)$$

the effective number of the relativistic degrees of freedom, is rather low – in accordance with our expectations related to the cosmic moduli problem [12]. Indeed, the total decay width of the (canonically normalized) sgoldstino

$$\Gamma_{\delta z} \simeq \Gamma_\theta + \Gamma_{\tilde{h}}, \quad (4.10)$$

where the individual decay widths are found to be

$$\Gamma_\theta \simeq \frac{\lambda_\theta^2 m_z^3}{32\pi m_P^2} \sqrt{1 - \frac{4m_\theta^2}{m_{3/2}^2}} \text{ and } \Gamma_{\tilde{h}} = \frac{2^{4v-1}}{3^{2v-1}} \lambda_\mu^2 \frac{\omega^2}{4\pi} \frac{m_z^3}{m_P^2} v^{4v}, \quad (4.11a)$$

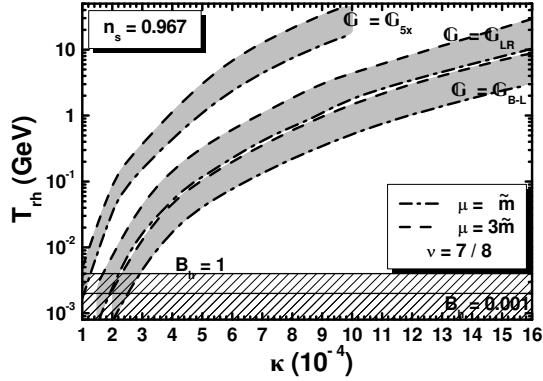


FIGURE 5: Allowed strips in the $\kappa - T_{\text{rh}}$ plane compatible with the inflationary requirements in Sec. 3.3 for $n_s = 0.967$, and various \mathbb{G} indicated in the graph. We take $\nu = 7/8$, and $\mu = \tilde{m}$ (dot-dashed lines) or $\mu = 3\tilde{m}$ (dashed lines). The BBN lower bounds on T_{rh} for hadronic branching ratios $B_h = 1$ and 0.001 are also depicted by two thin lines.

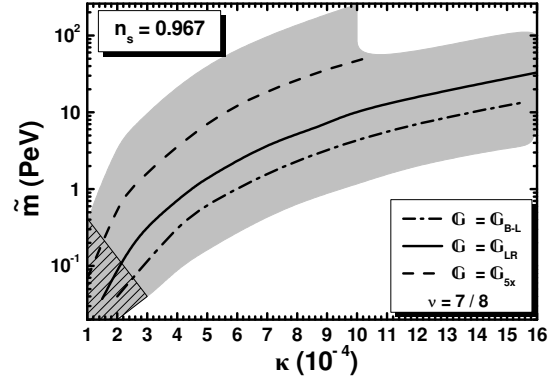


FIGURE 6: Region in the $\kappa - \tilde{m}$ plane allowed by the inflationary requirements in Sec. 3.3 for $n_s = 0.967$, $\tilde{m} \leq \mu \leq 3\tilde{m}$, $1 \leq N_G \leq 10$ and $3/4 < \nu < 1$. The allowed contours for $\nu = 7/8$ and specific \mathbb{G} are also depicted. Hatched is the region excluded by BBN for $B_h = 0.001$.

with $\lambda_\theta = \langle z \rangle / Nm_P = (4\nu - 3) / \sqrt{6}\nu$. From the expressions above we readily recognize that $\Gamma_{\delta z}$ is roughly proportional to m_z^3 / m_P^2 as expected for any typical modulus [12]. Selecting $\nu > 3/4$ we kinematically forbid the decay of δz into \tilde{G} 's and so we avoid the possible late decay of the produced \tilde{G} and the troubles with abundance of the subsequently produced lightest SUSY particles.

The compatibility between theoretical and observational values of light element abundances predicted by BBN entails [13] a lower bound on T_{rh} as follows

$$T_{\text{rh}} \geq 4.1 \text{ MeV for } B_h = 1 \text{ and } T_{\text{rh}} \geq 2.1 \text{ MeV for } B_h = 10^{-3}, \quad (4.12)$$

where B_h is the hadronic branching ratio and large $m_z \sim 0.1 \text{ PeV}$ is assumed.

Taking κ and m_z values allowed by the inflationary part of our model we find the allowed regions in $\kappa - T_{\text{rh}}$ plane, displayed in Fig. 5, for $\nu = 7/8$ and the various G considered here. The boundary curves of the allowed regions correspond to $\mu = \tilde{m}$ or $\lambda_\mu = 0.65$ (dot-dashed line) and $\mu = 3\tilde{m}$ or $\lambda_\mu = 1.96$ (dashed line). The $|\mu|/\tilde{m} - \lambda_\mu$ correspondence is determined via Eq. (4.7). We see that there is an ample parameter space consistent with the BBN bounds depicted by two horizontal lines. The maximal values of T_{rh} for the selected ν are obtained for $\mu = 3\tilde{m}$ and are estimated to be

$$T_{\text{rh}}^{\text{max}} \simeq \begin{cases} 14 \text{ GeV} & \text{for } \mathbb{G} = \mathbb{G}_{B-L}, \\ 33 \text{ GeV} & \text{for } \mathbb{G} = \mathbb{G}_{LR}, \\ 49 \text{ GeV} & \text{for } \mathbb{G} = \mathbb{G}_{5X}. \end{cases} \quad (4.13)$$

Obviously, reducing μ below \tilde{m} , the parameters λ_μ , $\Gamma_{\delta z}$, and so T_{rh} decrease too and the slice cut by the BBN bound increases. Therefore, our setting fits better with high-scale SUSY [14].

4.3 SUSY-MASS SCALE

Solving Eq. (3.6d) w.r.t m we obtain

$$m \simeq \left(\frac{a_S}{2^{1+\nu}(2-\nu)} \right)^{(2-\nu)/2} \left(\frac{3H_I^2}{(1-\nu)\nu^2} \right)^{\nu/4}. \quad (4.14)$$

Taking into account Eq. (3.3) which results $\langle z \rangle_I / m_P \sim 10^{-3} \ll 1$ we estimate $m \sim 10^3 a_S$. Inserting this result into Eq. (4.6a) and then into the rightmost relation of Eq. (4.7) we are able to gain information about \tilde{m} using as inputs the allowed a_S values in Eqs. (3.12a) – (3.12c) – which are compatible with the observational constraints to FHI. Since $a_S \sim 1$ TeV we expect $m \sim 1$ PeV, and so $\tilde{m} \sim 1$ PeV as well.

The qualitative arguments above are verified numerically in Fig. 6 where we delineate the gray shaded region allowed by the inflationary requirements of Sec. 3.3 for $n_s = 0.967$ by varying ν , μ and N_G within their possible respective margins

$$0.75 \lesssim \nu \lesssim 1, \quad 1 \lesssim \mu/\tilde{m} \lesssim 3 \quad \text{and} \quad 1 \leq N_G \leq 10. \quad (4.15)$$

Obviously the lower boundary curve of the displayed region is obtained for $\mathbb{G} = \mathbb{G}_{B-L}$ and $\nu \simeq 0.751$, whereas the upper one corresponds to $\mathbb{G} = \mathbb{G}_{5_X}$ and $\nu \simeq 0.99$. The hatched region is ruled out by Eq. (4.12). All in all, we obtain the predictions

$$1.2 \lesssim a_S/\text{TeV} \lesssim 460 \quad \text{and} \quad 0.09 \lesssim \tilde{m}/\text{PeV} \lesssim 253 \quad \text{with} \quad (4.16)$$

and $T_{\text{rh}}^{\text{max}} \simeq 71$ GeV, 139 GeV and 163 GeV for $\mathbb{G} = \mathbb{G}_{B-L}, \mathbb{G}_{LR}$ and \mathbb{G}_{5_X} respectively attained for $\mu = 3\tilde{m}$ and $\nu \simeq 0.99$. Fixing $\nu = 7/8$ and $\mu = \tilde{m}$, we obtain a prediction for \tilde{m} as a function of κ is depicted for the three \mathbb{G} 's considered in our work. We use the same type of lines as in Fig. 3. Assuming also that we can determine the segments of these lines that can be excluded by the BBN bound in Eq. (4.12). In all, we find that \tilde{m} turns out to be confined in the ranges

$$0.34 \lesssim \tilde{m}/\text{PeV} \lesssim 13.6 \quad \text{for} \quad \mathbb{G} = \mathbb{G}_{B-L}, \quad (4.17a)$$

$$0.21 \lesssim \tilde{m}/\text{PeV} \lesssim 32.9 \quad \text{for} \quad \mathbb{G} = \mathbb{G}_{LR}, \quad (4.17b)$$

$$0.58 \lesssim \tilde{m}/\text{PeV} \lesssim 46.8 \quad \text{for} \quad \mathbb{G} = \mathbb{G}_{5_X}. \quad (4.17c)$$

These results in conjunction with the necessity for $\mu \sim \tilde{m}$, established in Sec. 4.2 hint towards the PeV-scale MSSM. Our findings are compatible with the mass of the Higgs boson discovered in LHC [14] for degenerate sparticle spectrum $1 \leq \tan\beta \leq 50$ and varying the stop mixing.

4.4 GRAVITATIONAL WAVES FROM COSMIC STRINGS

When $\mathbb{G} = \mathbb{G}_{B-L}$, CSs may be produced after FHI with tension [4]

$$G\mu_{\text{cs}} \simeq \frac{1}{2} \left(\frac{M}{m_P} \right)^2 \varepsilon_{\text{cs}}(r_{\text{cs}}) \quad \text{with} \quad \varepsilon_{\text{cs}}(r_{\text{cs}}) = \frac{2.4}{\ln(2/r_{\text{cs}})} \quad \text{and} \quad r_{\text{cs}} = \kappa^2/8g^2 \leq 10^{-2}, \quad (4.18)$$

where we take into account that $(B-L)(\Phi) = 2$. Here $G = 1/8\pi m_P^2$ is the Newton gravitational constant and $g \simeq 0.7$ is the gauge coupling constant at a scale close to M . For the parameters in Eq. (3.12a) we find

$$0.59 \lesssim G\mu_{\text{cs}}/10^{-8} \lesssim 9.2. \quad (4.19)$$

If the CSs are *stable*, the corresponding parameter space is totally allowed by the level of the CS contribution to the observed anisotropies of CMB which is confined by *Planck* [15] in the range

$$G\mu_{\text{cs}} \lesssim 2.4 \cdot 10^{-7} \text{ at 95\% c.l.} \quad (4.20)$$

On the other hand, the results of Eq. (4.19) are completely excluded by the recent *Pulsar Timing Array* (PTA) bound which requires [16]

$$G\mu_{\text{cs}} \lesssim 2 \cdot 10^{-10} \text{ at 95\% c.l.} \quad (4.21)$$

However, if these CSs are *metastable* due to the embedding of \mathbb{G}_{B-L} into a larger gauge group, whose spontaneous breaking to \mathbb{G}_{B-L} produces monopoles – see e.g. Ref. [17, 18] –, an explanation of the PTA data on the stochastic background of GWs is possible for

$$0.9 \lesssim M/\text{TeV} \lesssim 2.56 \text{ and } 3 \lesssim \kappa/10^{-4} \lesssim 16. \quad (4.22)$$

Indeed, the obtained $G\mu_{\text{cs}}$ values, through Eq. (4.18), for the values above lie within the range dictated by the interpretation of the *NANOGrav 15-years data* (NG15) [16]

$$4.3 \cdot 10^{-8} \lesssim G\mu_{\text{cs}} \lesssim 2.4 \cdot 10^{-4} \text{ for } 8.2 \gtrsim \sqrt{r_{\text{ms}}} \gtrsim 7.5 \text{ at 95\% c.l.} \quad (4.23)$$

Here the metastability factor r_{ms} is the ratio of the monopole mass squared, m_{M}^2 , to μ_{cs} . Given that m_{M} is related to the symmetry breaking scale of the GUT covering \mathbb{G}_{B-L} , the rightmost restriction in Eq. (4.23) may constrain the relevant scale close to the M values in Eq. (4.22).

5. CONCLUSIONS

We analyzed the implementation of FHI together with the SUSY breaking within various GUTs in Eqs. (2.1a), (2.1b), and (2.1c). We adopted the super- and Kähler potentials in Eqs. (2.2) and (2.5) applying an approximate R symmetry. Our proposal offers the following worth-mentioning achievements:

- Observationally acceptable FHI adjusting the tadpole parameter, a_{S} , and the \mathbb{G} -breaking scale M ;
- A prediction of the SUSY-mass scale, \tilde{m} , which turns out to be of the order of PeV;
- Generation of the μ term of MSSM with $\mu \sim \tilde{m}$;
- An interpretation of the DE problem without extensive tuning;
- Compatibility of T_{rh} with BBN thanks to the considered μ values;
- An explanation of NG15 via the decay of metastable $B-L$ CSs if $\mathbb{G} = \mathbb{G}_{B-L}$.

A complete cosmological picture of our framework could be achieved if the issues of the correct baryon asymmetry and the cold-dark-matter abundance of the universe are also addressed.

REFERENCES

- [1] G.R. Dvali, Q. Shafi and R.K. Schaefer, *Large scale structure and supersymmetric inflation without fine tuning*, *Phys. Rev. Lett.* **73**, 1886 (1994) [hep-ph/9406319].
- [2] Y. Akrami *et al.* [Planck Collaboration], *Planck 2018 results. X. Constraints on inflation*, *Astron. Astrophys.* **641**, A10 (2020) [arXiv:1807.06211].
- [3] V.N. Şenoğuz and Q. Shafi, *Reheat temperature in supersymmetric hybrid inflation models*, *Phys. Rev. D* **71**, 043514 (2005) [hep-ph/0412102]; K. Nakayama *et al.*, *Constraint on the gravitino mass in hybrid inflation* *J. Cosmol. Astropart. Phys.* **12**, 010 (2010) [arXiv:1007.5152].
- [4] C. Pallis and Q. Shafi, *Update on Minimal Supersymmetric Hybrid Inflation in Light of PLANCK*, *Phys. Lett. B* **725**, 327 (2013) [arXiv:1304.5202].
- [5] W. Buchmüller, V. Domcke, K. Kamada and K. Schmitz, *Hybrid Inflation in the Complex Plane*, *J. Cosmol. Astropart. Phys.* **07**, 054 (2014) [arXiv:1404.1832].
- [6] R. Armillis and C. Pallis, *Implementing Hilltop F-term Hybrid Inflation in Supergravity*, “Recent Advances in Cosmology”, edited by A. Travena and B. Soren (Nova Science Publishers Inc., New York, 2013) [arXiv:1211.4011].
- [7] G. Lazarides and C. Pallis, *Probing the Supersymmetry-Mass Scale With F-term Hybrid Inflation*, *Phys. Rev. D* **108**, no. 9, 095055 (2023) [arXiv:2309.04848].
- [8] C. Pallis, *PeV-Scale SUSY and Cosmic Strings from F-Term Hybrid Inflation*, *Universe* **10**, no. 5, 211 (2024) [arXiv:2403.09385].
- [9] C. Pallis, *Gravity-mediated SUSY breaking, R symmetry, and hyperbolic Kähler geometry*, *Phys. Rev. D* **100**, no. 5, 055013 (2019) [arXiv:1812.10284]; C. Pallis, *SUSY-breaking scenarios with a mildly violated R symmetry*, *Eur. Phys. J. C* **81**, no. 9, 804 (2021) [arXiv:2007.06012].
- [10] N. Aghanim *et al.* [Planck Collaboration], *Planck 2018 results. VI. Cosmological parameters*, *Astron. Astrophys.* **641**, A6 (2020); *Erratum: Astron. Astrophys.* **652**, C4 (2021) ([arXiv:1807.06209].
- [11] M. Tristram *et al.*, *Improved limits on the tensor-to-scalar ratio using BICEP and Planck*, *Phys. Rev. Lett.* **127**, 151301 (2021) [arXiv:2112.07961].
- [12] K.J. Bae, H. Baer, V. Barger and R.W. Deal, *The cosmological moduli problem and naturalness*, *J. High Energy Phys.* **02**, 138 (2022) [arXiv:2201.06633].
- [13] T. Hasegawa *et al.*, *MeV-scale reheating temperature and thermalization of oscillating neutrinos by radiative and hadronic decays of massive particles*, *J. Cosmol. Astropart. Phys.* **12**, 012 (2019) [arXiv:1908.10189].
- [14] E. Bagnaschi, G.F. Giudice, P. Slavich and A. Strumia, *Higgs Mass and Unnatural Supersymmetry*, *J. High Energy Phys.* **09**, 092 (2014) [arXiv:1407.4081].
- [15] P.A.R. Ade *et al.* [Planck Collaboration], *Planck 2015 results. XIII. Cosmological parameters* *Astron. Astrophys.* **594**, A13 (2016) [arXiv:1502.01589].
- [16] A. Afzal *et al.* [NANOGrav Collaboration], *The NANOGrav 15 yr Data Set: Search for Signals from New Physics*, *Astrophys. J. Lett.* **951**, no. 1, L11 (2023); *ibid.* **971**, no. 1, L27 (2024) [arXiv:2306.16219].
- [17] S.F. King, G.K. Leontaris and Y.L. Zhou, *Flipped SU(5): unification, proton decay, fermion masses and gravitational waves*, *J. High Energy Phys.* **03**, 006 (2024) [arXiv:2311.11857].
- [18] W. Ahmed, T.A. Chowdhury, S. Nasri and S. Saad, *Gravitational waves from metastable cosmic strings in Pati-Salam model in light of new pulsar timing array data*, *Phys. Rev. D* **109**, no. 1, 015008 (2024) [arXiv:2308.13248].